Journal of Power Sources 297 (2015) 252–259

Contents lists available at ScienceDirect

Journal of Power Sources

journal homepage: www.elsevier.com/locate/jpowsour

AC power generation from microbial fuel cells

Fernanda Leite Lobo [1], Heming Wang [1], Casey Forrestal, Zhiyong Jason Ren [*]

Department of Civil, Environmental, and Architectural Engineering, University of Colorado Boulder, Boulder, CO 80309, USA

HIGHLIGHTS

- First study on AC voltage in 1 Hz, 10 Hz and 60 Hz from MFCs.
- 95% efficiency DC–AC converter for MFCs.
- No energy storage needed for low voltage AC power from MFCs.

ARTICLE INFO

Article history:
Received 20 June 2015
Received in revised form
18 July 2015
Accepted 29 July 2015
Available online 10 August 2015

Keywords:
Microbial fuel cell
DC–AC converter
AC power
Frequency

ABSTRACT

Microbial fuel cells (MFCs) directly convert biodegradable substrates to electricity and carry good potential for energy-positive wastewater treatment. However, the low and direct current (DC) output from MFC is not usable for general electronics except small sensors, yet commercial DC–AC converters or inverters used in solar systems cannot be directly applied to MFCs. This study presents a new DC–AC converter system for MFCs that can generate alternating voltage in any desired frequency. Results show that AC power can be easily achieved in three different frequencies tested (1, 10, 60 Hz), and no energy storage layer such as capacitors was needed. The DC–AC converter efficiency was higher than 95% when powered by either individual MFCs or simple MFC stacks. Total harmonic distortion (THD) was used to investigate the quality of the energy, and it showed that the energy could be directly usable for linear electronic loads. This study shows that through electrical conversion MFCs can be potentially used in household electronics for decentralized off-grid communities.

1. Introduction

The microbial fuel cell (MFC) technology has been intensively researched due to its unique capability of converting any biodegradable substrates, especially waste materials, into renewable electricity [1,2]. MFCs carry good potential to transform traditional energy intensive wastewater treatment into energy-neutral or even energy-positive processes, but it requires a quantum change in technological advances in scale, cost, and practicality [3–5]. In addition to retrofit existing large-scale wastewater treatment, MFCs can be an ideal waste treatment and renewable energy solution for decentralized or remote villages in a nearer term, because it provides both energy and sanitation infrastructures for these communities [6].

The technology downside is the low power production at current stage. Despite great progress made in reactor configuration, material and operation that improved power output from 1 mW m^{-2} to about 19 W m^{-2}, the voltage provided by MFCs is still in the order of mV [7]. This is why energy harvesting using power electronics is crucial to make MFC application relevant. To date all efforts in MFC energy harvesting have been focusing on direct current (DC) output using DC–DC converters [8–10], capacitor charging and discharging [11–13] and power management systems [14,15]. These systems have been developed to boost the voltage to power small electronic devices such as hydrophones or sensors [14,16,17], and a recent study provides a comprehensive review of the current status and future need of practical energy harvesting from MFCs [7].

While in many cases DC output is sufficient for MFC-powered sensor applications, alternating current (AC) power generation is needed for community waste treatment and power solutions, because general household electrical appliances require AC power to operate, and the electrical grid distributes the electricity in the form of AC. Other renewable energy source such as Solar also produces DC power, which is then converted to AC power using

* Corresponding author.
E-mail address: jason.ren@colorado.edu (Z.J. Ren).
[1] These authors are equal contribution.

http://dx.doi.org/10.1016/j.jpowsour.2015.07.103
0378-7753/

Nomenclature

a_h, b_h	Fourier Coefficients (V)
C	Capacitance (F)
f	Frequency (Hz)
FFT	Fast Fourier Transform
h	Harmonic Order
I_{MFC}	MFC Current (I)
RMS	Root Mean Square
R_{output}	Output Resistor (Ω)
T	Period (seconds)
V_{MFC}	MFC Voltage (V)
V_n	N^{th} Harmonic Order Voltage (V)
V_{output}	Output Voltage (V)
$V(t)$	Voltage function over time (V)
X_c	Capacitor Impedance (Ω)
ω	Fundamental Frequency (radians)

inverter or DC–AC converter. The DC–AC converters are commercially sold but require an input voltage of at least 12 V [18], far beyond MFC voltage output level.

Though AC power generation from MFCs has not been reported so far, it becomes an imminent need for larger scale MFC development to meet real-world requirements. In this study, AC power generation was realized from MFCs through the development of a DC–AC converter system, and AC power in different frequencies with different MFC input voltages were also investigated. In addition, the quality of energy and the efficiency of the converter were also examined. Different frequency and quality investigations are important because unlike DC power, AC power outputs vary among different regions in the world. For example, Europe adopts an AC standard of 220–240 V at 50 Hz, while North America uses 120 V at 60 Hz.

2. Materials and methods

2.1. MFC construction and operation

Single-chamber MFCs were built by one polycarbonate cube-shaped chamber with an empty volume of 28 mL. A heat-treated graphite brush was used as the anode, and 30% water-proof carbon cloth (7 cm^2, Fuel Cell Earth) was as the air-cathode, which composed of one carbon base layer, four polytetrafluoroethylene diffusion layers and one catalyst layer (0.5 mg Pt cm^{-2}) [19]. MFCs were inoculated with anaerobic sludge obtained from the Boulder Water Resource Recovery Facility. The growth medium contains (per liter) 1.0 g CH_3COONa, 0.31 g NH_4Cl, 0.13 g KCl, 3.32 g $NaH_2PO_4 \cdot 2H_2O$, 10.32 g $Na_2HPO_4 \cdot 12H_2O$, 12.5 mL mineral solution, and 5 mL vitamin solution [20]. Fresh medium was refilled every 24 h. All MFCs were run in duplicate in batch mode at room temperature.

2.2. DC to AC circuit design and control

The custom-designed DC–AC converter is able to transform MFC DC power output to AC output (Fig. 1). The DC–AC converter consists of MFCs (MFC1 and MFC2) as the DC power sources, capacitors (C1 and C2, 1000 μF) as the intermediate energy storage, and MOSFETs (M1 and M2, NTD4906N) as switches. The switches M1 and M2 were alternately controlled ON/OFF in order to create positive and negative parts of the AC outputs. The control signals to switch ON/OFF were programmed by an Arduino microcontroller (Uno, R2) which was connected to a laptop. A binary value of 1 (5 V)

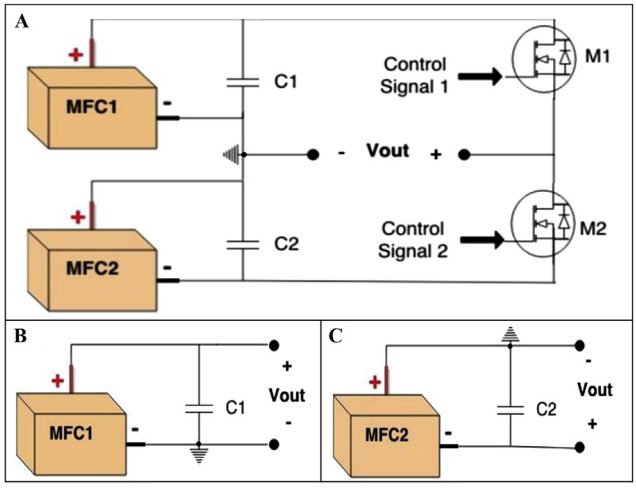

Fig. 1. (A) Circuit diagram of the DC–AC converter system for MFCs; (B) equivalent circuit diagram when MOSFET M1 is ON and MOSFET M2 is OFF to output the positive part of AC; (C) equivalent circuit diagram when MOSFET M1 is OFF and MOSFET M2 is ON to output the negative part of AC.

assigned by the Arduino turns on the MOSFET while a binary value of 0 (0 V) turns off the MOSFET. Since the control signal is a pulse with a period (T) that is equal to the sum of T_{ON} and T_{OFF}, and the period of a signal is the inverse of the frequency (f) or $T = 1/f$, it can be derived that $T_{ON} = T_{OFF} = 1/2f$. The DC–AC converter was tested in different conditions, including three different frequencies (1 Hz, 10 Hz and 60 Hz), absence or presence of energy storage layers (capacitors), and powered by 2 MFCs or 4 MFCs paired in series. Serial MFC connection provides higher voltages and more power for the DC–AC converter.

2.3. Analyses

The control signals for M1 and M2, the voltages and electrode potentials of the MFCs, the output voltage of the DC–AC converter, and the current in the circuit were all measured using an Oscilloscope (Agilent Technologies, DS01024A). MFC polarization curves were measured by varying external resistors from open circuit to 50 Ω using a resistor box.

To evaluate the efficiency of the DC–AC converter, a 100 kΩ resistor was used as the output load to close the circuit but simulate open circuit condition. The efficiency of the DC–AC converter was calculated by Equation (1):

$$\eta = \frac{V_{output}^2}{R_{output}} \frac{1}{V_{MFC}\, I_{MFC}} 100\% \quad (1)$$

where V_{output} is the root mean square (RMS) value of the AC output voltage that represents the usable voltage in AC, since the output voltage is a square wave, its RMS value is the same as the maximum value [21]; R_{output} is the output resistor which equals 100 kΩ; V_{MFC} and I_{MFC} are the voltage and current from the MFC, respectively, and I_{MFC} is the same as the current passing through the output resistor (100 kΩ) (Fig. 1B and C). Using an electrochemical workstation may provide more accurate I_{MFC} value and such method will be performed in future studies.

3. Results and discussion

3.1. Operation of the DC–AC converter under different frequencies

The DC–AC converter was operated by an Arduino

microcontroller, which generates control signals to turn ON or OFF the MOSFETs at desired frequencies (1 Hz, 10 Hz, or 60 Hz in this study). Fig. 1A shows the schematic diagram of the DC–AC converter. When M1 is ON and M2 is OFF, the DC voltage from MFC1 passes through while the DC voltage from MFC2 is cut off, so the MFC1 DC voltage is mirrored as the positive part of the AC voltage (Fig. 1B); In contrast, when M1 is OFF and M2 is on, DC voltage in opposite direction is generated from M2 through the converter, which is mirrored as the negative part of the AC voltage (Fig. 1C). As a result, the output voltages of the DC–AC converter continuously alternate between positive and negative voltages in periodic cycles, that is, AC voltages.

To test the feasibility of applying different frequencies, control signals for each MOSFET (M1 and M2) were operated at frequencies of 1 Hz, 10 Hz and 60 Hz (Fig. 2). The frequency of 60 Hz (Fig. 2C) is the primary goal because most electric loads are operated at 60 Hz AC. The frequencies of 1 Hz (Fig. 2A) and 10 Hz (Fig. 2B) were chosen to demonstrate that the DC–AC converter can work at various frequencies under different MFC performance. All the control signals are periodic square waves with a period of $T = 1/f$, where half of the period (T_{ON}) has a binary value of 1 (5 V) and the other half of the period (T_{OFF}) has a binary value of 0 (0 V). Since the period of the control signal depends on the frequency, the period decreased from 1 Hz to 60 Hz, as shown in Fig. 2A–C.

3.2. AC power output without using energy storage layer (capacitors)

Most MFC harvesting systems use energy storages, such as capacitors, due to the low direct energy output from MFCs. For this experiment, the energy storage layer was avoided in order to simplify the circuit and investigate if MFCs can power DC–AC converter directly and effectively (Fig. 3). Two MFCs or four MFCs (2 groups of 2 MFCs in series) were used as the direct DC power inputs. Without using capacitors as the energy storage layer, DC power from MFCs was successfully transformed to AC power. The AC voltage outputs kept square-shaped waves at 1 Hz and 10 Hz and only slightly deformed at 60 Hz. The input DC voltages and the output AC voltages both dropped gradually with increasing the frequency from 1 Hz to 60 Hz, but the output AC voltages were always comparable to the input DC voltages. When the DC–AC converter was powered by two MFCs, the positive AC outputs decreased along with the increase of frequency. For example, the AC outputs decreased from 720 mV (1 Hz) to 680 mV (10 Hz) and then to 480 mV (60 Hz), and the absolute values of the negative AC outputs decreased from 600 mV (1 Hz) to 560 mV (10 Hz) and then to 400 mV (60 Hz). Similar trend was observed under 4-MFC conditions, with the positive AC outputs decreased from 1480 mV (1 Hz) to 1280 mV (10 Hz) and 1000 mV (60 Hz), and the absolute values of the negative AC outputs decreased from 1320 mV (1 Hz) to 1160 mV (10 Hz) and 880 mV (60 Hz).

The slope of the linear section on the polarization curve has been widely used to determine the internal resistance of the direct output of an MFC [22]. Similar concepts can be adopted in AC condition. Fig. S1 shows that the polarization curves under different frequencies can be considered as parallel lines without significant slope changes, which means that the internal resistances of MFC1 and MFC2 kept consistent when energy-harvesting frequencies changed. The internal resistances of MFC1 and MFC2 were estimated as 41.7 ± 1 Ω and 48 ± 2 Ω at the three frequencies, respectively.

MFC anode and cathode potentials were measured to investigate the influence of frequencies on the MFC voltage. When the frequency increased from 1 Hz to 10 Hz then to 60 Hz, anode potentials were comparable while cathode potentials significantly dropped. The open circuit cathode potentials of MFC1 and MFC2

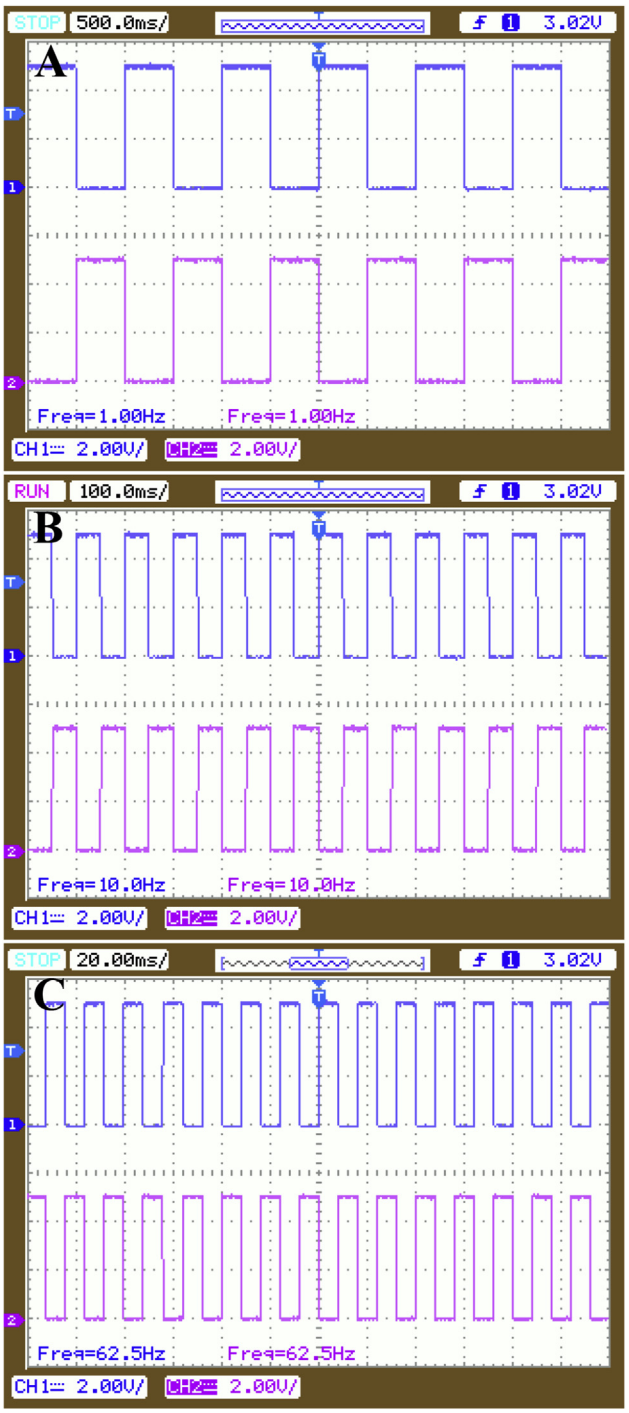

Fig. 2. Control signals at 1 Hz (A), 10 Hz (B) and 60 Hz (C). The blue curve is the control signal for MOSFET M1 and the magenta curve is the control signal for MOSFET M2. (For interpretation of the references to colour in this figure legend, the reader is referred to the web version of this article.)

decreased from 232 mV to 88 mV and from 216 mV to 48 mV, respectively, while the open circuit anode potentials remained at 464 ± 20 mV for all the three frequencies (Fig. 4). The comparable anode potentials among different frequencies suggested that enough electrons were available for current generation because of the capacitive properties of the anodic biofilm [23,24]. The decrease of cathode potentials is hypothesized due to local pH increase, which were reported by previous studies that OH^- accumulation on the Pt-based air cathode can cause a potential loss up to 0.3 V

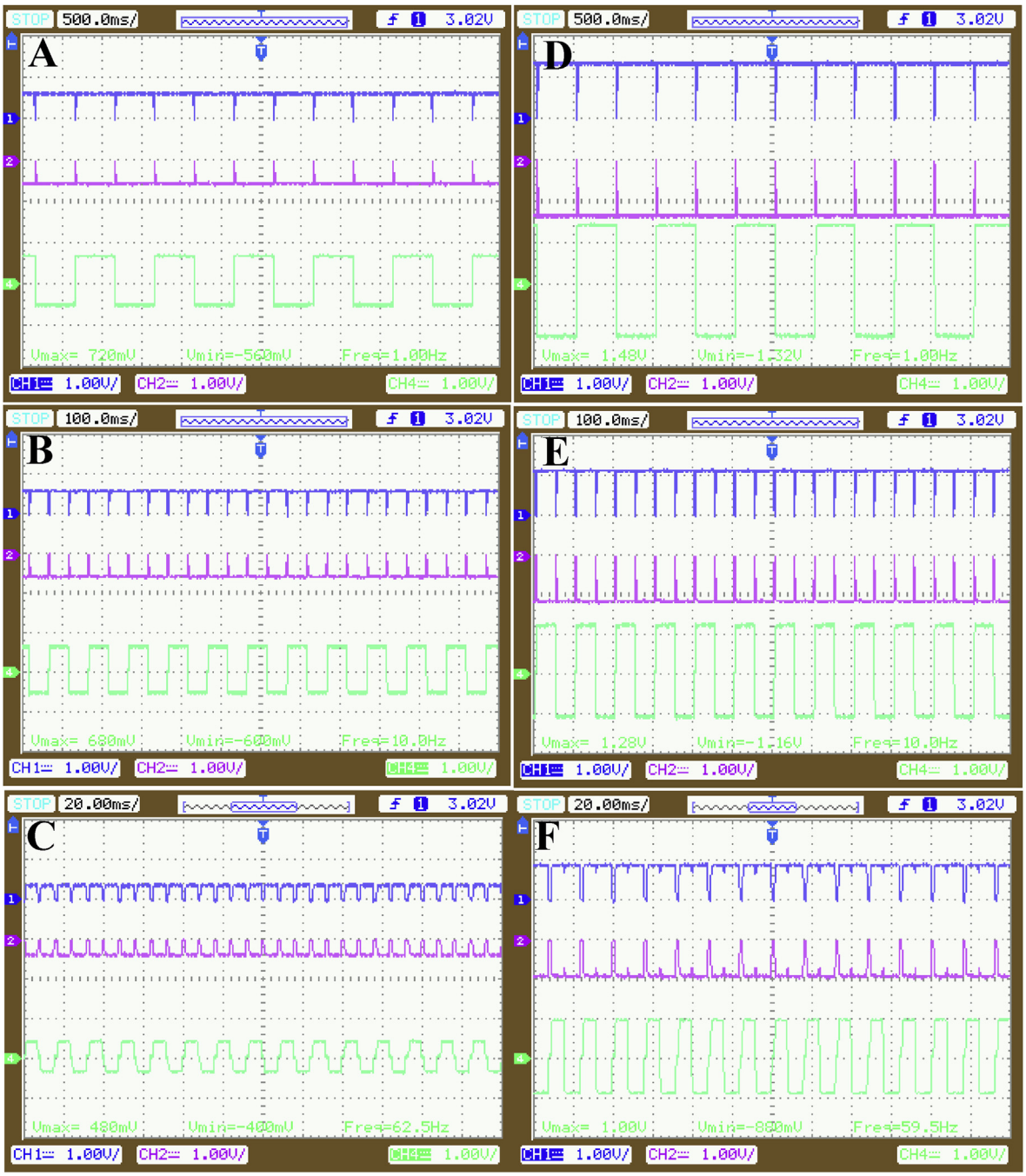

Fig. 3. Input and output voltages without using energy storage layer (capacitors) in the circuit. The DC–AC converter was powered by two MFCs at 1 Hz (A), 10 Hz (B) and 60 Hz (C) or four MFCs (2 groups of 2 MFCs in series) at 1 Hz (D), 10 Hz (E) and 60 Hz (F). Blue waves: MFC1; magenta waves: MFC2; green waves: AC output. (For interpretation of the references to colour in this figure legend, the reader is referred to the web version of this article.)

[25]. During higher frequency energy-harvesting, the transport of OH^- to the bulk electrolyte is slower than lower frequencies because of the smaller T_{ON} and T_{OFF}, which may cause potential drop due to limited mass transfer. No pH change was observed in bulk solution due to the use of buffer solution, but more studies are needed to further investigate the cathode potential drops at different energy-harvesting frequencies with local pH measurements on the electrode surface.

3.3. AC power output with energy storage layer (capacitors)

To compare with the results without using energy storage layer, in following studies we added capacitors in the circuit as temporary energy storage to transform DC power from MFCs to AC power outputs from the converter. Similar MFC connections were used (2 MFCs or 4 MFCs in 2 × 2 serial connection), but the results in terms of shape and magnitude are very different between the two scenarios with or without capacitors (Fig. 3 vs. Fig. 5). Compared with regular shaped AC square waves when no capacitors were used, the input and output waves were distorted at even 1 Hz when capacitors were present and the waves became even indistinguishable at 60 Hz. In addition, the input DC voltages and output AC voltages dropped significantly with capacitors in the circuit from 1 Hz to 60 Hz. The positive AC outputs decreased from 680 mV

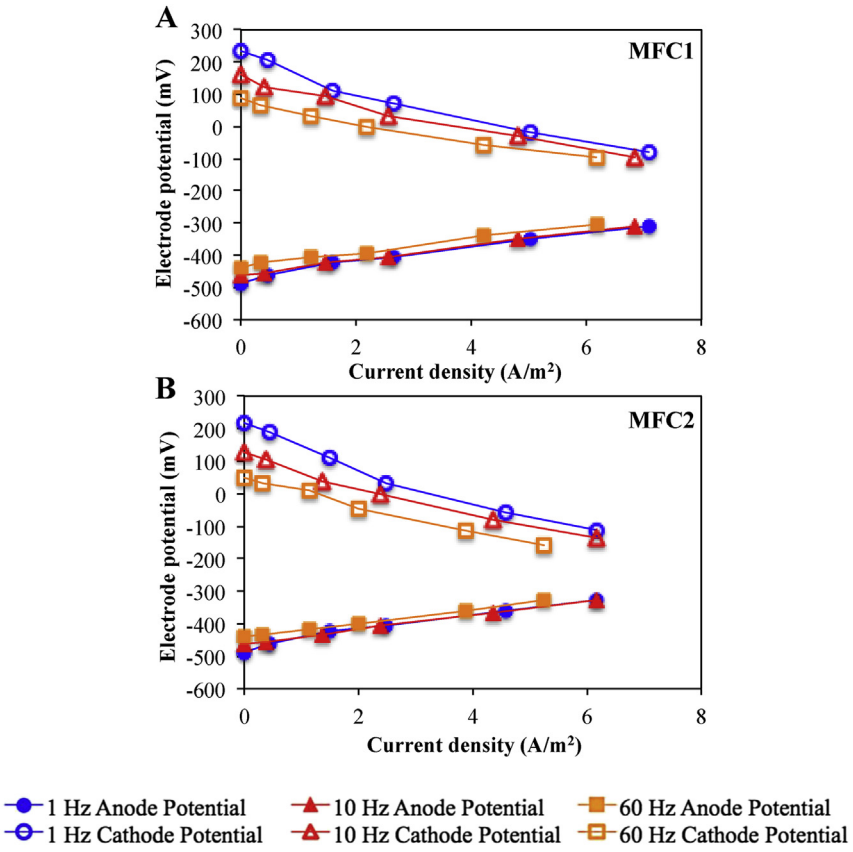

Fig. 4. Electrode potential changes of MFC1 (A) and MFC2 (B) at frequencies of 1 Hz, 10 Hz and 60 Hz without using capacitors in the circuit.

(1 Hz) to 120 mV (60 Hz) when powered by 2 MFCs and from 1160 mV (1 Hz) to −40 mV (60 Hz) when powered by 4 MFCs. The absolute values of the negative AC outputs decreased from 600 mV (1 Hz) to 40 mV (60 Hz) when powered by 2 MFCs and from 1040 mV (1 Hz) to 160 mV (60 Hz) when powered by 4 MFCs.

When comparing the output AC voltages at the same frequency, we found that the AC outputs were much lower when capacitors were used, especially under the conditions of higher frequencies. At 1 Hz, the output voltage decreased only 40 mV (from 720 mV to 680 mV) when the DC–AC converter was powered by 2 MFCs (Fig. 3A vs. 5A), and a higher drop was observed (320 mV) when 4 MFCs were used (Fig. 3D vs. 5D). At 10 Hz, such drops increased to 320 mV (2 MFCs) and 1000 mV (4 MFCs), respectively (Fig. 3B vs. 5B, Fig. 3E vs. 5E). Similarly, even bigger drops were observed under 60 Hz, with 360 mV and 1400 mV dropped under the 2-MFC or 4-MFC condition, respectively (Fig. 3C vs. 5C, Fig. 3F vs. 5F).

The big drop of output AC voltage when capacitors were added was believed due to the impedance of capacitors at different frequencies. The impedance of a capacitor (Xc) changes according to the frequency (f, Hz) and its capacitance (C, F), with the relationship expressed as [26].

$$Xc = \frac{1}{2\pi fC} \tag{2}$$

When the frequency increases from 1 Hz to 10 Hz and 60 Hz, the impedance of the capacitor decreases from $Xc_{1Hz} = 160\ \Omega$ to $Xc_{10Hz} = 16\ \Omega$, and then to $Xc_{60Hz} = 2.6\ \Omega$, based on Equation (2). The capacitor works as a low-pass filter as it cuts the voltage components for the higher frequencies and let only the voltage components of the low frequency pass through [26]. The low-pass filter is a voltage divider between the resistance of the circuit and the impedance of the capacitor (Supporting information for more details). Therefore, the voltage across the capacitor, which is mirrored to the output voltage, drops along the decreasing impedance and increasing frequencies. To avoid this performance drop, the capacitor should be determined according to the desired frequency. For instance, if the desired frequency is 60 Hz, a capacitor with a smaller capacitance of around 20 μF should be chosen to create a greater impedance of around 160 Ω. This study chose a capacitor of 1000 μF, which is more compatible with 1 Hz, and that's why less drop was found under 1 Hz while large drop was found under 60 Hz.

3.4. AC power quality from MFCs

In conventional AC electric energy systems, the voltage generated is a sine waveform with a frequency of 60 Hz (U S.). During the transformation from renewable DC power to AC power, like those from solar panels or MFCs in this study, the power quality, expressed as total harmonic distortion (THD) at 60 Hz, depends on how the AC voltage generated via the DC–AC converter differs from the conventional 60 Hz sine wave voltages. In other words, the power quality is related to the quantity of harmonics in the AC voltage generated via the DC–AC converter. A harmonic is a sinusoidal waveform with a frequency that is an integral multiple of the fundamental frequency of 60 Hz [27]. The THD measures the quantity of harmonics of a wave by using Fourier analysis, via which any periodic waveforms can be described as an infinite sum of sine waves in different frequencies (Supporting information for more details). Since the output voltage from the DC–AC converter is a

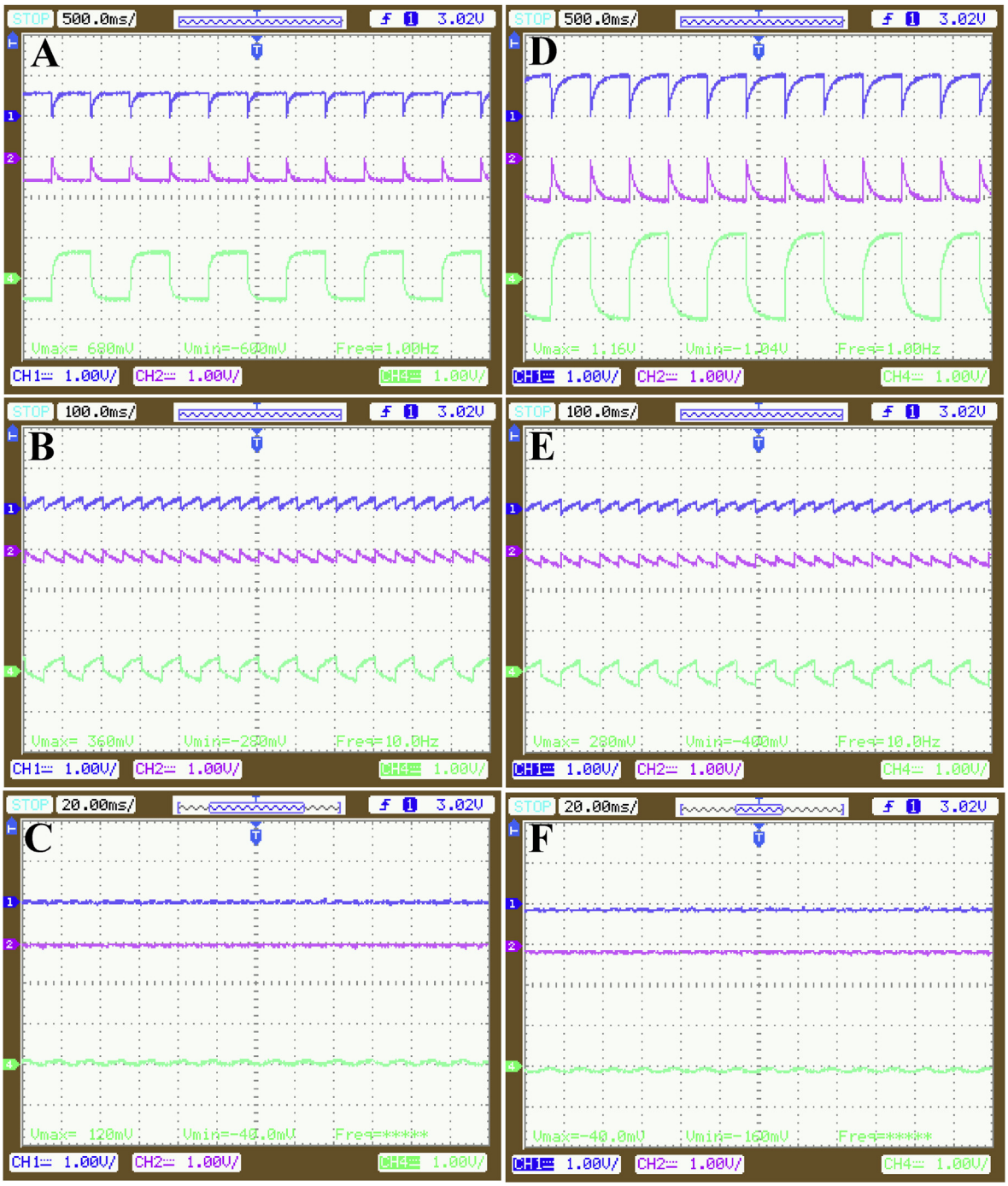

Fig. 5. Input and output voltages when using energy storage layer (capacitors) in the circuit. The DC–AC converter was powered by two MFCs at 1 Hz (A), 10 Hz (B) and 60 Hz (C) or four MFCs (2 groups of 2 MFCs) in series at 1 Hz (D), 10 Hz (E) and 60 Hz (F). Blue waves: MFC1; magenta waves: MFC2; green waves: AC output. (For interpretation of the references to colour in this figure legend, the reader is referred to the web version of this article.)

periodic waveform with period T, thus it can be described as [21].

$$V(t) = \frac{1}{T}\int_0^T V(t)dt + \sum_{h=1}^{h=+\infty}[a_h \cos(h\omega t) + b_h \sin(h\omega t)] \quad (3)$$

where h is the harmonic order, ω is the fundamental frequency that is equal to $2\pi/T$ and a_h and b_h are given by

$$a_h = \frac{2}{T}\int_0^T V(t)\cos(h\omega t)dt \quad (4)$$

$$b_h = \frac{2}{T}\int_0^T V(t)\sin(h\omega t)dt \quad (5)$$

The harmonic order is the multiple of the fundamental frequency, for instance, the second harmonic for a fundamental

frequency of 60 Hz is at the frequency of 120 Hz.

The Fast Fourier Transform (FFT) is an algorithm that represents the Fourier analysis in the frequency domain, which can easily provide the voltage in each harmonic. The THD is measured by Ref. [21].

$$THD = \frac{\sqrt{V_2^2 + V_3^2 + V_4^2 + \ldots + V_n^2}}{V_1} 100\% \quad (6)$$

where V_1 is the voltage in the fundamental frequency, V_2 is the voltage in the second harmonic, V_3 is the voltage in the third harmonic and so on.

The FFT of the output voltages were measured when the DC–AC converter was powered by 2 MFCs (Fig. 6A) or 4 MFCs (Fig. 6B) at 60 Hz, which is the standard frequency of AC in the electric power grid in the U.S. When the DC–AC converter was powered by 2 MFCs, the most relevant harmonic was the third harmonic, where the frequency (180 Hz) was three times as the fundamental frequency. The corresponding THD of the output voltage was around 30%. When 4 MFCs were used, the most relevant harmonics were the second (120 Hz) and third harmonic (180 Hz), with a relevant THD around 30% as well. The THD standard for grid-tied systems is 8% [28], but for stand-alone renewable systems the square-wave DC–AC converter with a THD of 30%, like the one developed here, can be used to power linear loads safely [21].

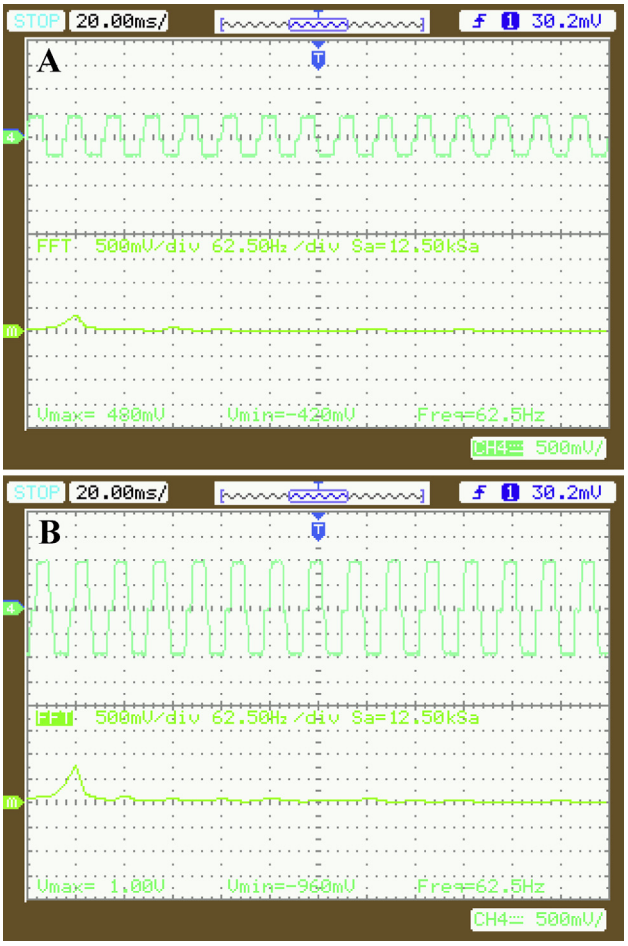

Fig. 6. Output voltages and the Fast Fourier Transform (FFT) of the output voltages at 60 Hz when the DC–AC converter was powered by two MFCs (A) and four MFCs (2 groups of 2 MFCs in series) (B).

3.5. The efficiency of the DC–AC converter

The efficiency of the DC–AC converter was calculated without using the capacitors in the circuit (Fig. 7). The custom-designed DC–AC converter was very efficient with the efficiencies reached almost 100% in repeated tests. The efficiencies of the DC–AC converter among various frequencies (1 Hz, 10 Hz, and 60 Hz) were around 97 ± 3%, with the limited energy losses mainly due to the MOSFET conduction loss and the switching loss. When the frequencies increased from 1 Hz to 60 Hz, the efficiencies decreased because more energy was lost on the MOSFET switches at the high switching frequency, but the energy loss was still small. When the DC–AC converter was powered by 4 MFCs instead of 2 MFCs, the average efficiencies were slightly higher (99 ± 1%) due to higher voltage and more power provided. This result encourages the potential that if enough MFCs connected in series to provide a DC voltage of 110 V, the energy loss can be manageable. Since the microcontroller was not the focus in this study, the overall efficiency of the circuit including the extra power for Arduino was not investigated.

3.6. Discussion

This study proves that AC power can be efficiently generated from microbial fuel cells, and different frequencies can be varied depending on the needs of electronic loads. The first DC–AC converter for MFCs has efficiency above 95%, which can assist the development of MFC systems for power and sanitation solutions for decentralized communities. Although the low voltage provided directly from MFCs is not enough to power an electric load, this study shows that MFC stacks may be able to do so without significant energy loss. In addition, transformers can be coupled at the output of the DC–AC converter to boost the voltage to a usable level.

However, many challenges remain before large-scale systems can be developed to power electric loads, such as potential voltage reversal in MFC stacks and more efficiency energy harvesting from MFC reactors. Maximum power point tracking (MPPT) algorithms and many other approaches are being investigated to solve these problems [29,30]. In addition, the voltage output in this studied DC–AC converter topology is based on a mirror control of the input voltage provided by the MFC. By using a different control scheme like modified sine-wave Pulse Width Modulation (PWM), the quality of energy output can be even higher. Also, because MFC DC voltage output can vary constantly due to the change of environmental conditions, a closed loop control in the converter may be applied to improve the output voltage stability.

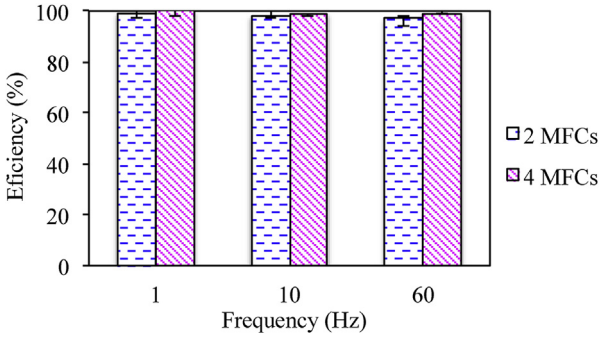

Fig. 7. Efficiency of the DC–AC converter powered by two or four MFCs (2 groups of 2 MFCs in series) at 1 Hz, 10 Hz and 60 Hz.

Acknowledgement

We thank the financial support from CAPES (Science without Borders) for FLL and Office of Naval Research (Award N000141310901) for HW and ZJR.

Appendix A. Supporting information

Supporting information related to this article can be found at http://dx.doi.org/10.1016/j.jpowsour.2015.07.103.

References

[1] B. Logan, K. Rabaey, Conversion of wastes into bioelectricity and chemicals by using microbial electrochemical technologies, Science 337 (2012) 686–690.
[2] H. Wang, Z.J. Ren, A comprehensive review of microbial electrochemical systems as a platform technology, Biotechnol. Adv. 31 (2013) 1796–1807.
[3] R.A. Rozendal, H.V.M. Hamelers, K. Rabaey, J. Keller, C.J.N. Buisman, Towards practical implementation of bioelectrochemical wastewater treatment, Trends Biotechnol. 26 (2008) 450–459.
[4] T.H.J.A. Sleutels, A. Ter Heijne, C.J.N. Buisman, H.V.M. Hamelers, Bioelectrochemical systems: an outlook for practical applications, ChemSusChem 5 (2012) 1012–1019.
[5] H. Wang, H. Luo, P.H. Fallgren, S. Jin, Z.J. Ren, Bioelectrochemical system platform for sustainable environmental remediation and energy generation, Biotechnol. Adv. 33 (2015) 317–334.
[6] H. Yazdi, L. Alzate-Gaviria, Z.J. Ren, Pluggable microbial fuel cell stacks for septic wastewater treatment and electricity production, Bioresour. Technol. 180 (2015) 258–263.
[7] H. Wang, J.-D. Park, Z.J. Ren, Practical energy harvesting for microbial fuel cells: a review, Environ. Sci. Technol. 49 (2015) 3267–3277.
[8] N. Degrenne, B. Allard, F. Buret, S.-E. Adami, D. Labrousse, C. Vollaire, et al., A 140 mV self-starting 10 mW DC/DC converter for powering low-power electronic devices from low-voltage microbial fuel cells, J. Low Power Electron. 8 (2012) 485–497.
[9] J.-D. Park, Z. Ren, Hysteresis-controller-based energy harvesting scheme for microbial fuel cells with parallel operation capability, Energy Convers. IEEE Trans. 27 (2012) 715–724.
[10] N. Degrenne, F. Buret, F. Morel, S.E. Adami, D. Labrousse, B. Allard, et al., Self-starting DC: DC boost converter for low-power and low-voltage microbial electric generators, in: IEEE Energy Convers. Congr. Expo. Energy Convers. Innov. A Clean Energy Futur. ECCE 2011, Proc., 2011, pp. 889–896.
[11] A. Dewan, H. Beyenal, Z. Lewandowski, Intermittent energy harvesting improves the performance of microbial fuel cells, Environ. Sci. Technol. 43 (2009) 4600–4605.
[12] P. Liang, W. Wu, J. Wei, L. Yuan, X. Xia, X. Huang, Alternate charging and discharging of capacitor to enhance the electron production of bioelectrochemical systems, Environ. Sci. Technol. 45 (2011) 6647–6653.
[13] S. Ren, X. Xia, L. Yuan, P. Liang, X. Huang, Enhancing charge harvest from microbial fuel cells by controlling the charging and discharging frequency of capacitors, Bioresour. Technol. 146 (2013) 812–815.
[14] M. Alaraj, Z.J. Ren, J.-D. Park, Microbial fuel cell energy harvesting using synchronous flyback converter, J. Power Sources 247 (2014) 636–642.
[15] C. Donovan, A. Dewan, H. Peng, D. Heo, H. Beyenal, Power management system for a 2.5 W remote sensor powered by a sediment microbial fuel cell, J. Power Sources 196 (2011) 1171–1177.
[16] Y. Gong, S.E. Radachowsky, M. Wolf, M.E. Nielsen, P.R. Girguis, C.E. Reimers, Benthic microbial fuel cell as direct power source for an acoustic modem and seawater oxygen/temperature sensor system, Environ. Sci. Technol. 45 (2011) 5047–5053.
[17] A. Shantaram, H. Beyenal, R. Raajan, A. Veluchamy, Z. Lewandowski, Wireless sensors powered by microbial fuel cells, Environ. Sci. Technol. 39 (2005) 5037–5042.
[18] ABB micro inverter system, (n.d.). http://www05.abb.com/global/scot/scot232.nsf/veritydisplay/7efd88eadccaa1c585257dc5006e334e/$file/MICRO-0.25-0.3-0.3HV-Rev1.6.pdf. (accessed 10.12.14).
[19] H. Wang, D. Heil, Z.J. Ren, P. Xu, Removal and fate of trace organic compounds in microbial fuel cells, Chemosphere 125 (2015) 94–101.
[20] H. Zhu, H. Wang, Y. Li, W. Bao, Z. Fang, C. Preston, et al., Lightweight, conductive hollow fibers from nature as sustainable electrode materials for microbial energy harvesting, Nano Energy 10 (2014) 268–276.
[21] R.W. Erickson, D. Maksimovic, Fundamentals of Power Electronics, second ed., Kluwer Academic Publishers, New York, 2001.
[22] B.E. Logan, B. Hamelers, R. Rozendal, U. Schroder, Microbial fuel cells: methodology and technology, Environ. Sci. Technol. 40 (2006) 5181–5192.
[23] H. Wang, Z. Ren, J.-D. Park, Power electronic converters for microbial fuel cell energy extraction: effects of inductance, duty ratio, and switching frequency, J. Power Sources 220 (2012) 89–94.
[24] Z. Lu, P. Girguis, P. Liang, H. Shi, G. Huang, L. Cai, et al., Biological capacitance studies of anodes in microbial fuel cells using electrochemical impedance spectroscopy, Bioprocess Biosyst. Eng. 38 (2015) 1325–1333.
[25] X. Wang, C. Feng, N. Ding, Q. Zhang, Accelerated OH−transport in activated carbon air cathode by modification of quaternary ammonium for microbial fuel cells, Environ. Sci. Technol. 48 (2014) 4191–4198.
[26] C.K. Alexander, M.N.O. Sadiku, Fundamentals of Electric Circuit, fifth ed., McGraw-Hill, New York, 2013.
[27] R.D. Henderson, P.J. Rose, Harmonics: the effects on power quality and transformers, IEEE Trans. Ind. Appl. 30 (1994).
[28] IEEE Power and Energy Society, IEEE recommended practice and requirements for harmonic control in electric power systems, IEEE Power Energy Soc. (2014) https://standards.ieee.org/findstds/standard/519-2014.html.
[29] H.C. Boghani, G. Papaharalabos, I. Michie, K.R. Fradler, R.M. Dinsdale, A.J. Guwy, et al., Controlling for peak power extraction from microbial fuel cells can increase stack voltage and avoid cell reversal, J. Power Sources 269 (2014) 363–369.
[30] H. Wang, J.-D. Park, Z. Ren, Active energy harvesting from microbial fuel cells at the maximum power point without using resistors, Environ. Sci. Technol. 46 (2012) 5247–5252.